

755 (1971).

¹⁸J. Lefrançois, Rapporteur's talk given at the International Symposium on Electron and Photon Interactions at High Energies, Cornell University, 1971 (unpublished).

¹⁹P. Lindenfeld, A. Sachs, and J. Steinberger, Phys. Rev. **89**, 531 (1953); C. P. Sargent, R. Cornelius, M. Rinehart, L. M. Lederman, and K. Rogers, Phys. Rev. **98**, 1349 (1955); Yu. A. Budagov, S. Wiktor, V. P. Dzhepelov, P. F. Ermolov, and V. I. Moskalev, Zh. Eksp. i Teor. Fiz. **38**, 1047 (1960) [Sov. Phys. JETP **11**, 755 (1960)]; N. P. Samios, Phys. Rev. **121**, 275 (1961); S. Devons, P. Nemethy, C. Nissim-Sabat, E. di Capua, and A. Lanzara, Phys. Rev. **184**, 1356 (1969).

²⁰J. Parisi, thèse de troisième cycle, Paris, 1970

(unpublished); J. Parisi and P. Kessler, in *Fourth International Symposium on Electron and Photon Interactions at High Energies, Liverpool, 1969*, edited by D. W. Braben and R. E. Rand (Daresbury Nuclear Physics Laboratory, Daresbury, Lancashire, England, 1970), p. 289; report, 1969 (unpublished); Lett. Nuovo Cimento **2**, 760 (1971).

²¹J. Parisi and P. Kessler, following paper, Phys. Rev. D **5**, 2237 (1972).

²²J. M. Jauch and F. Rohrlich, *The Theory of Photons and Electrons* (Addison-Wesley, Cambridge, Mass., 1955), p. 237. See also F. Mandl and T. H. R. Skyrme, Proc. Roy. Soc. (London) **A215**, 497 (1952).

PHYSICAL REVIEW D

VOLUME 5, NUMBER 9

1 MAY 1972

Investigation of the Vertices $\pi^0\gamma\gamma$, $\eta\gamma\gamma$, and $\eta'\gamma\gamma$ with Electron-Positron Storage Rings. II*

J. Parisi

Laboratoire de Physique Générale, Faculté des Sciences de l'Université VI de Paris, Paris, France

and

P. Kessler

Laboratoire de Physique Atomique, Collège de France, Paris, France

(Received 9 December 1971)

We here suggest an experimental investigation of the $X\gamma\gamma$ vertices ($X = \pi^0$, η , or η') in the specific case where both photons are spacelike, one of them being almost real and the other one highly virtual. For this purpose, we suggest that, in an electron-positron storage ring, e^-e^+ inelastic collisions of the type $e^-e^+ \rightarrow e^-e^+X \rightarrow e^-e^+\gamma\gamma$ should be analyzed, one of the outgoing e^\pm particles being detected at a very small scattering angle (a few milliradians), in coincidence with the other one measured at a relatively large scattering angle (higher than a few degrees) and with both decay photons emitted at large angle with respect to the beam axis. Assuming various experimental cutoffs on angles and energies, we show that (a) the background due to double bremsstrahlung can be made negligible through our choice of these cutoffs; (b) for $X = \pi^0$ or η , the cross sections should be high enough to justify experiments of this type to be planned with future storage rings of beam energy ≥ 3 GeV and luminosity $\geq 10^{32}$ cm⁻² sec⁻¹; (c) such experiments should allow a discrimination between various types of electromagnetic form factors used for the $X\gamma\gamma$ vertices.

I. INTRODUCTION

In a recent paper,¹ we suggested an investigation of the $X\gamma\gamma$ vertices ($X = \pi^0$, η , η') in electron-positron storage rings, using the process $e^-e^+ \rightarrow e^-e^+X \rightarrow e^-e^+\gamma\gamma$ under specific experimental conditions which should be the following: Both outgoing e^\pm particles would be detected at very small scattering angles, in coincidence with both photons produced at large angles with respect to the beam axis. Such an experiment should allow a quite precise measurement of the various $X\gamma\gamma$ coupling constants [or, equivalently, of the decay widths $\Gamma(X \rightarrow 2\gamma)$]. This suggestion inserted itself into the general scheme defined in our previous papers^{2,3}

for studying photon-photon collisions through inelastic e^-e^+ scattering processes (and in particular reactions of the type $e^-e^+ \rightarrow e^-e^+A^-A^+$, where A^\pm is any charged particle) in electron-positron colliding-beam devices.

We here suggest the following variant of the experimental scheme proposed before: Only one of the outgoing e^\pm particles would be detected at a very small scattering angle (not more than a few milliradians), whereas the other one would be measured at a relatively large scattering angle (at least a few degrees). Thus, only one of the virtual spacelike photons exchanged [see the Feynman diagram of Fig. 1(a)] would be almost real [its q^2 value would be lower than a few (MeV/c)² for beam

energies of a few GeV], whereas the other one would be highly virtual [its q^2 value would be higher than 10^4 (MeV/c) 2]. The basic purpose of such an experiment would be to determine the electromagnetic form factors of the $X\gamma\gamma$ vertices in a spacelike region.

This type of experiment was already proposed and studied by the authors two years ago,⁴ but not in an entirely realistic way. In particular, we assumed at the time that a missing-mass experiment (measuring only the outgoing e^\pm particles) would be sufficient, whereas we now consider that, in order to get a sure identification of the pseudo-scalar particle X , the decay photons from the process $X \rightarrow 2\gamma$ (which is the only one existing in the case $X = \pi^0$, the most important one for $X = \eta$, and still the simplest one for $X = \eta'$) should also be measured.

Before showing our numerical predictions, we first present a check – extracted from our preliminary work⁴ – of the Williams-Weizsäcker approximation⁵ which we used throughout in our calculations and which is much discussed nowadays.⁶

We then study the problem of background rejection, this background being due – as in Ref. 1 – to the double-bremsstrahlung process, the leading term of which is represented by the diagram of

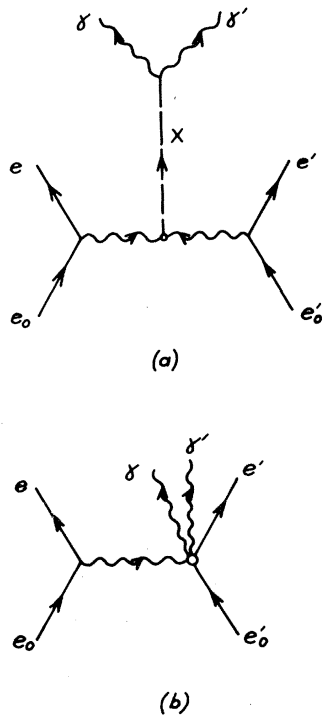


FIG. 1. (a) Main Feynman diagram for the process $e^-e^+ \rightarrow e^-e^+X \rightarrow e^-e^+\gamma\gamma$ ($X = \pi^0, \eta, \text{ or } \eta'$). (b) Leading Feynman diagram (under the conditions defined) for the double-bremsstrahlung process $e^-e^+ \rightarrow e^-e^+\gamma\gamma$.

Fig. 1(b). We will show that this background can be made negligible by imposing additional experimental requirements. At the same time, we give the values of the integrated cross sections of the process of interest, and we show that – under the conditions assumed – these values are sufficient, at least for $X = \pi^0$ and η , to ensure reasonable counting rates with e^-e^+ storage rings of beam energy ≥ 3 GeV and luminosity $\geq 10^{32}$ cm $^{-2}$ sec $^{-1}$.

We also show the angular dependence of the cross sections (with respect to the e^\pm particle scattered at large angle), and in particular the influence of various types of electromagnetic form factors proposed for the $X\gamma\gamma$ vertices.

In our conclusion, we rediscuss briefly the interest and feasibility of such experiments, and we mention their connection with some recent suggestions for e^\pm colliding-beam experiments made by other authors.

Details of calculation are given in an Appendix.

II. CHECK OF THE WILLIAMS-WEIZSÄCKER METHOD

In order to check the Williams-Weizsäcker approximation,⁵ we calculated, for the process $e^-e^+ \rightarrow e^-e^+\pi^0$, the differential cross section $d\sigma/[2\pi d(\cos\theta')]$, divided by the width Γ of the π^0 , using both an exact calculation and the approximation, the latter being applied to the vertex where an e^\pm particle is scattered at a small angle (for simplicity, we shall call this vertex the left-hand one). θ' is the scattering angle of the right-hand e^\pm particle (supposed to be scattered at a comparatively large angle; i.e., $\theta' \geq 5^\circ$). For the left-hand scattering angle, we chose a higher limit $\theta_{\max} = 3^\circ$. In both the exact formula [(A9) in the Appendix] and the approximate formula (A16), the electromagnetic form factor F was assumed to depend only on the four-momentum squared ($t' = |q'^2$) of the right-hand virtual photon. Three different expressions were used for this form factor, namely:

$$F_1 = 1, \quad F_2 = (1 + t'/0.77)^{-1}, \quad F_3 = (1 + t'/0.71)^{-2},$$

with t' expressed in (GeV/c) 2 .

Figures 2(a), 2(b), and 2(c) show the curves obtained, with these three form factors, for beam energies $E_0 = 1, 2, \text{ and } 3$ GeV, respectively. It can be seen that, when compared with the exact calculation, the Williams-Weizsäcker approximation always gives the right order of magnitude and angular behavior, even at $E_0 = 3$ GeV, where the four-momentum transfer ($|q^2|^{1/2}$) of the left-hand vertex can no longer be considered as very small with respect to the pion mass [we then have ($|q^2|_{\max}^{1/2} \cong 150$ MeV/c)]. Thus the approximation

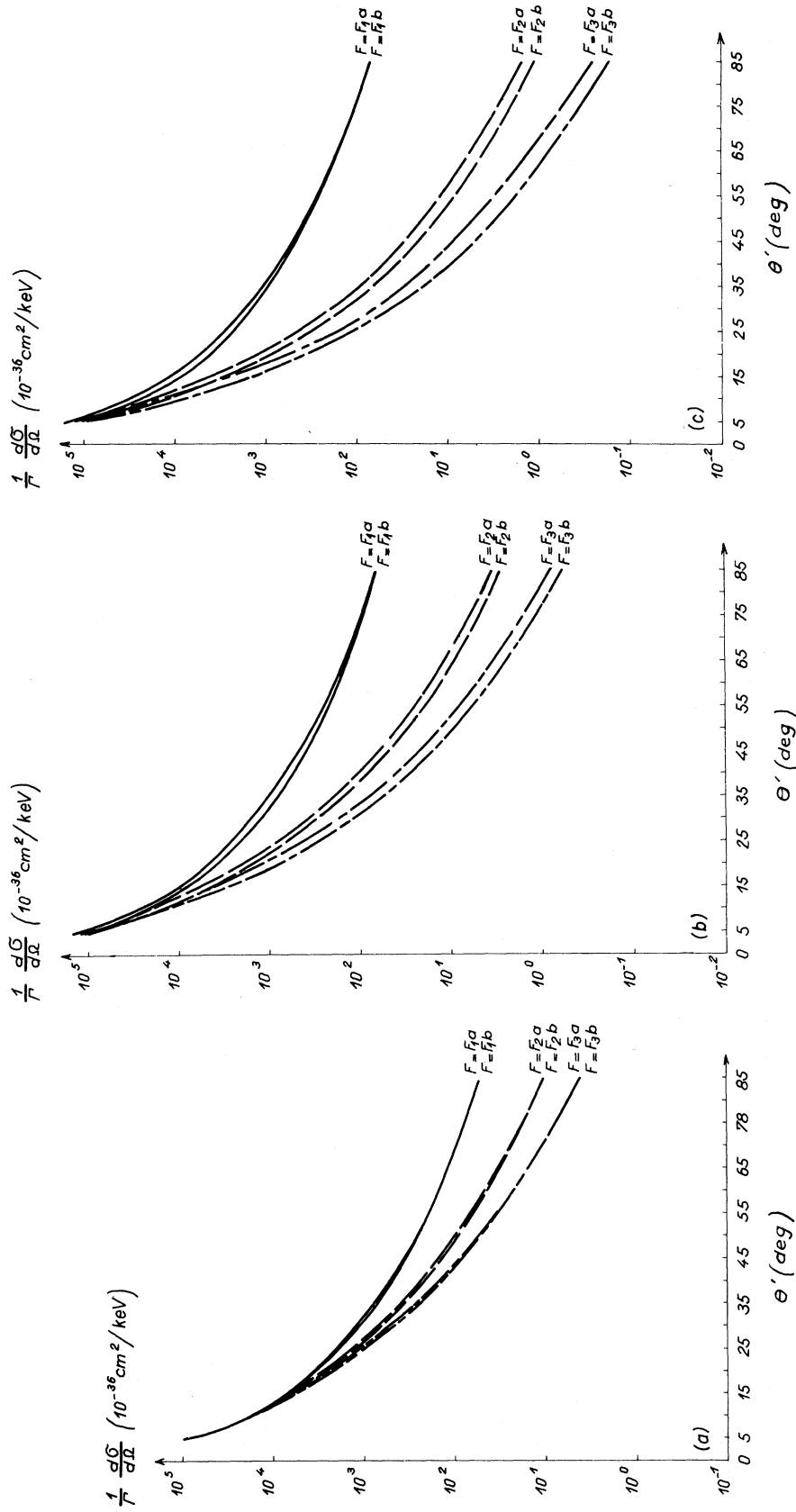


FIG. 2. Comparison between an exact calculation and the Williams-Weizsäcker approximation for the differential cross section $d\sigma/d\Omega$ [$d\Omega = 2\pi d(\cos\theta')$], where θ' is the scattering angle of the right-hand e^\pm particle, i.e., that scattered at large angle], divided by the decay width $\Gamma(\pi^0 \rightarrow 2\gamma)$, considering only the process $e^-e^+ \rightarrow e^-e^+\pi^0$. The maximal scattering angle of the left-hand (almost forward scattered) e^\pm particle was taken as $\theta_{\max} = 3^\circ$. (a) $E_0 = 1$ GeV, (b) $E_0 = 2$ GeV, (c) $E_0 = 3$ GeV. *a*: Williams-Weizsäcker approximation; *b*: exact calculation.

works even better than we might have expected. On the other hand, it is legitimate to assume that this approximation would work still better for those reactions of the same type where particles with higher masses (η and η') are produced. Finally, since in our following study we take an even much smaller value of θ_{\max} (only 4 mrad), we may conclude that our use of the Williams-Weizsäcker approximation in that study was perfectly justified, and that the errors involved should not be higher than a few percent.

III. BACKGROUND ELIMINATION AND VALUES OF INTEGRATED CROSS SECTIONS

In order to introduce realistic experimental conditions for the study of the reaction $e^-e^+ \rightarrow e^-e^+X \rightarrow e^-e^+\gamma\gamma$ according to the variant considered here [diagram of Fig. 1(a), with the left-hand virtual photon almost real and the right-hand one highly virtual], we define the following parameters (see the kinematic scheme of Fig. 3 for the definition of the scattering and emission angles):

(i) A maximal scattering angle θ_{\max} for the left-hand e^\pm particle; we chose 4 mrad as the standard value for θ_{\max} .

(ii) A minimal emission angle ψ_{\min} for both outgoing photons; more precisely, this means that $\psi_{\min} \leq \psi$, $\psi' \leq \pi - \psi_{\min}$. We took $\psi_{\min} = 45^\circ$.

(iii) A minimal scattering angle θ'_{\min} for the right-hand e^\pm particle. We chose $\theta'_{\min} = 5^\circ$.

(iv) A maximal scattering angle θ'_{\max} for the right-hand e^\pm particle. We chose $\theta'_{\max} = 35^\circ$, so that $\theta'_{\max} < \psi_{\min}$. This choice was motivated both by theoretical reasons (background rejection, see the discussion in Sec. III of Ref. 1) and by experimental ones (it appears preferable that the devices for photon detection and for e^\pm detection should be located in separate angular regions).

(v) A maximal relative energy loss $\chi_{\min} (= \omega_{\min}/E_0)$, ω being the energy of the left-hand virtual photon), imposed to the left-hand e^\pm particle. The values to be chosen for χ_{\min} will be discussed hereafter.

(vi) A maximal relative energy loss χ_{\max}

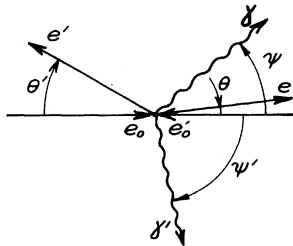


FIG. 3. Kinematic scheme corresponding to Figs. 1(a) and 1(b) (for simplicity, azimuthal angles are left out).

($= \omega_{\max}/E_0$) for the left-hand e^\pm particle. The standard value chosen was $\chi_{\max} = 70\%$.

It should be noticed that here there is no reason for defining similar cutoffs on the relative energy loss of the right-hand e^\pm particle. However, an absolute lower limit of 10 MeV was set on the energy E' of the outgoing right-hand e^\pm particle.

On the other hand, we used the following values of partial decay rates, branching ratios, and masses:

(1) Partial decay rates $\Gamma(X \rightarrow 2\gamma)$: 11 eV for X

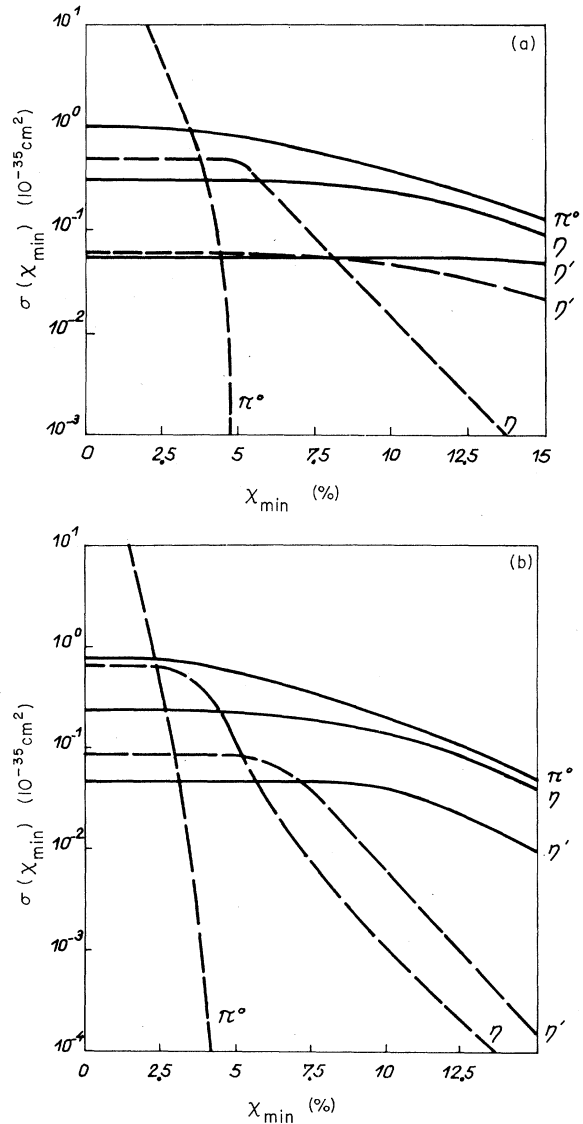


FIG. 4. Integrated cross section as a function of χ_{\min} , for the process $e^-e^+ \rightarrow e^-e^+X \rightarrow e^-e^+\gamma\gamma$, with $\theta_{\max} = 4$ mrad, $\theta'_{\min} = 5^\circ$, $\theta'_{\max} = 35^\circ$, $\psi_{\min} = 45^\circ$, $\chi_{\max} = 70\%$. (a) $E_0 = 2$ GeV, (b) $E_0 = 3$ GeV. Solid lines, main process (form factor $F = F_3$); dashed lines, background, i.e., double bremsstrahlung with the 2γ invariant mass integrated over between $m_X - 100$ MeV and $m_X + 100$ MeV.

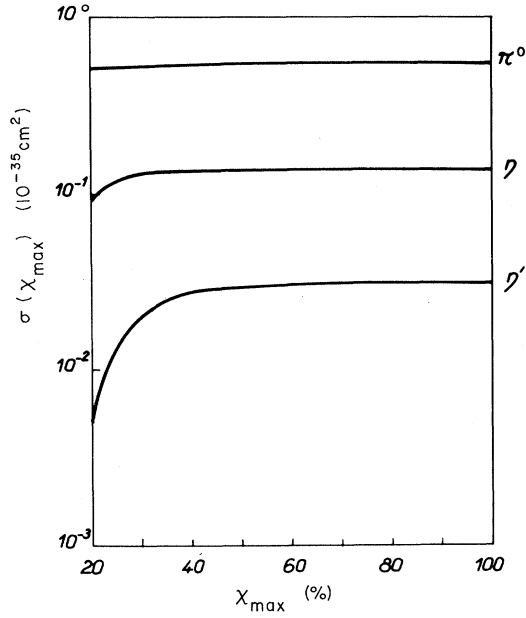


FIG. 5. Integrated cross section as a function of χ_{\max} , for the process $e^-e^+ \rightarrow e^-e^+X \rightarrow e^-e^+\gamma\gamma$, with $E_0 = 3$ GeV; $\theta_{\max} = 4$ mrad, $\theta'_{\min} = 5^\circ$, $\theta'_{\max} = 35^\circ$; $\psi_{\min} = 45^\circ$; $\chi_{\min} = 5\%$ for $X = \pi^0$, 13% for $X = \eta$, 20% for $X = \eta'$. (Form factor $F = F_3$.)

$= \pi^0, {}^8 1$ keV for $X = \eta, {}^8 5$ keV for $X = \eta'$ (which is just a guess, assuming that this rate is approximately proportional to m_X^3).

(2) Branching ratios $\Gamma(X \rightarrow 2\gamma)/\Gamma(X \rightarrow \text{total})$: 100% for π^0 , 40% for $\eta, {}^9 10\%$ for η' .¹⁰

(3) Masses m_X : 135 MeV for π^0 , 549 MeV for η , 958 MeV for η' .

The first point we studied was the variation of the integrated cross sections with χ_{\min} , for both

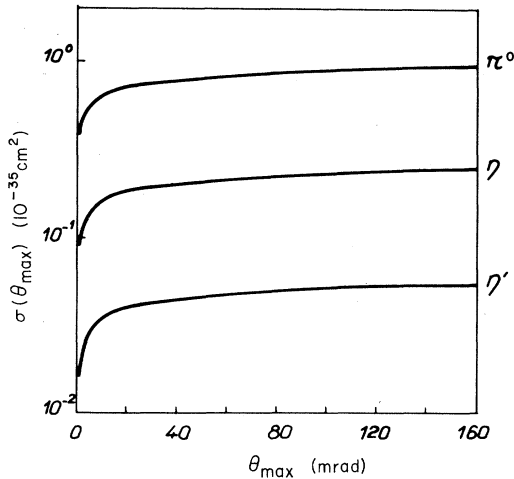


FIG. 6. Integrated cross section as a function of θ_{\max} , for the process $e^-e^+ \rightarrow e^-e^+X \rightarrow e^-e^+\gamma\gamma$, with $E_0 = 3$ GeV; $\theta'_{\min} = 5^\circ$; $\theta'_{\max} = 35^\circ$; $\psi_{\min} = 45^\circ$; $\chi_{\min} = 5\%$ for $X = \pi^0$, 13% for $X = \eta$, 20% for $X = \eta'$; $\chi_{\max} = 70\%$. (Form factor $F = F_3$.)

the main term [Fig. 1(a)] and the background [Fig. 1(b)]. The corresponding curves are shown in Figs. 4(a) and 4(b) for $E_0 = 2$ GeV and 3 GeV, respectively; here all cutoff parameters other than χ_{\min} were kept fixed at their standard values. For the main term, the electromagnetic form factor

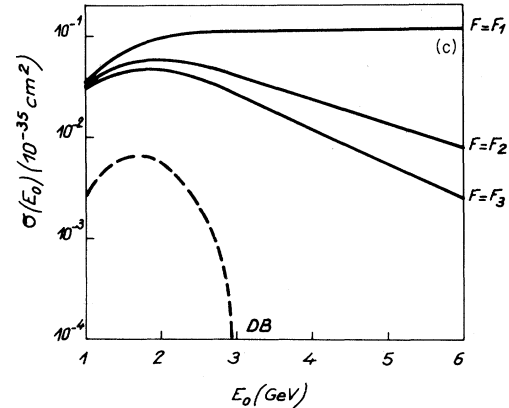
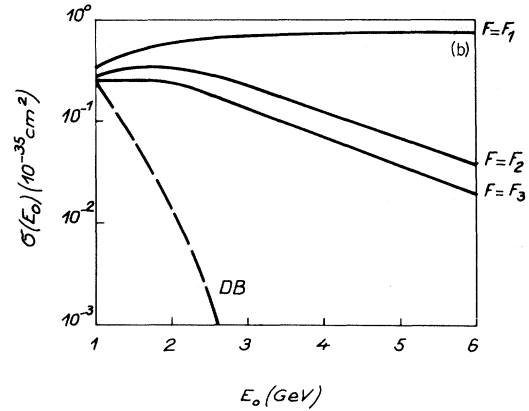
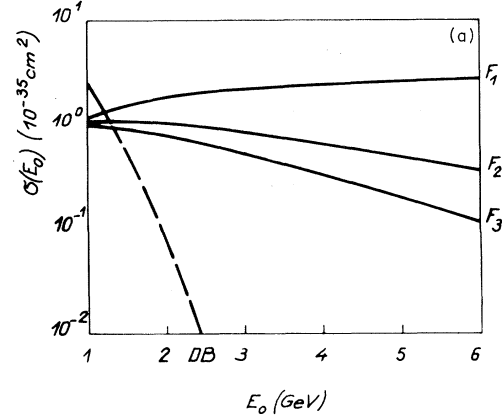


FIG. 7. Integrated cross section as a function of E_0 , for the process $e^-e^+ \rightarrow e^-e^+X \rightarrow e^-e^+\gamma\gamma$, with $\theta_{\max} = 4$ mrad; $\theta'_{\min} = 5^\circ$; $\theta'_{\max} = 35^\circ$; $\psi_{\min} = 45^\circ$; $\chi_{\max} = 70\%$ (a) $X = \pi^0$, $\chi_{\min} = 5\%$. (b) $X = \eta$, $\chi_{\min} = 13\%$. (c) $X = \eta'$, $\chi_{\min} = 20\%$. Solid lines, main process ($F = F_1, F_2$, or F_3); dashed line, background, i.e., double bremsstrahlung with the 2γ invariant mass integrated over between $m_X - 100$ MeV and $m_X + 100$ MeV.

TABLE I. Integrated cross sections in 10^{-35} cm², calculated for the process $e^-e^+ \rightarrow e^-e^+X \rightarrow e^-e^+\gamma\gamma$, with $\theta_{\max} = 4$ mrad, $\theta'_{\min} = 5^\circ$, $\theta'_{\max} = 35^\circ$, $\psi_{\min} = 45^\circ$, $\chi_{\max} = 70\%$.

$E_0 =$	$X = \pi^0$ ($\chi_{\min} = 5\%$)		$X = \eta$ ($\chi_{\min} = 13\%$)		$X = \eta'$ ($\chi_{\min} = 20\%$)	
	3 GeV	4 GeV	3 GeV	4 GeV	3 GeV	4 GeV
$F = F_1$	2.36	2.61	0.66	0.67	0.11	0.11
$F = F_2$	0.87	0.65	0.22	0.13	0.04	0.02
$F = F_3$	0.54	0.34	0.14	0.06	0.03	0.01

F_3 (as defined in Sec. II) was used, in order to give a lower rather than a higher limit for the cross sections. In the background term, the 2γ invariant mass was integrated over between $m_X - \Delta m$ and $m_X + \Delta m$ with $\Delta m = 100$ MeV. It can be seen that (a) the background rejection is substantially better at $E_0 = 3$ GeV than at 2 GeV; (b) as the mass of X gets higher, higher values of χ_{\min} must be chosen in order to ensure an efficient background suppression. We were thus led to adopt the following standard values: $\chi_{\min} = 5\%$ for π^0 , 13% for η , and 20% for η' .

We then studied the variation of the integrated cross sections of the main term with χ_{\max} (Fig. 5) and θ_{\max} (Fig. 6), all other cutoff parameters being kept fixed at their standard values, the beam energy being taken as $E_0 = 3$ GeV, and the electromagnetic form factor F_3 being chosen. It is seen that both χ_{\max} and θ_{\max} are not critical parameters.

Finally, we studied the energy behavior of the integrated cross sections [Figs. 7(a), 7(b), and 7(c) for $X = \pi^0$, η , and η' , respectively], all cutoff parameters being kept at their standard values.

The effect of the three electromagnetic form factors defined in Sec. II is shown. Also shown is the energy behavior of the background; here again we notice that the background suppression becomes much better when the energy is increased.

In Table I, we show the numerical values obtained for the integrated cross sections of the main term at $E_0 = 3$ GeV and 4 GeV, all cutoff parameters being kept fixed at their standard values, and the three form factors F_1 , F_2 , F_3 being used.

To conclude, let us mention that all numerical integrations were performed, using formulas (A16) and (A20) of the Appendix (for the main term and the background term, respectively), through a computer program (the limitations on the angle ψ' had to be introduced specially into the program, since this angle is not used as an integration variable).

IV. ANGULAR DEPENDENCE

We show, in Figs. 8(a), 8(b), 8(c), the differential cross section $d\sigma/d(\cos\theta')$ of the main process,

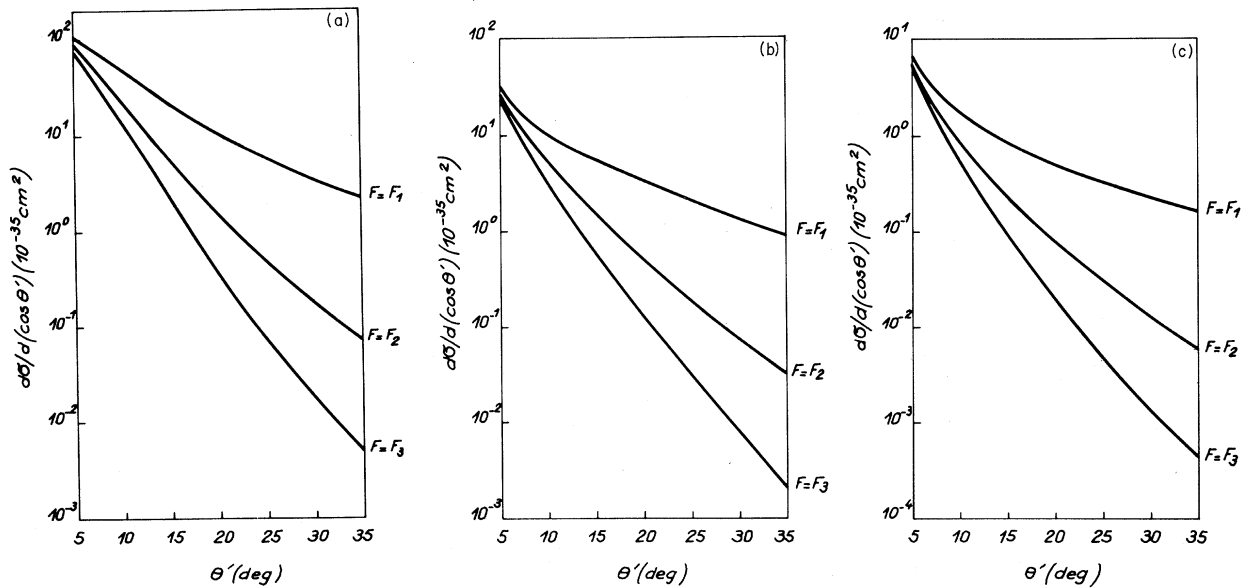


FIG. 8. Differential cross section $d\sigma/d(\cos\theta')$ for the process $e^-e^+ \rightarrow e^-e^+X \rightarrow e^-e^+\gamma\gamma$, with $E_0 = 3$ GeV, $\theta_{\max} = 4$ mrad, $\psi_{\min} = 45^\circ$, $\chi_{\max} = 70\%$. (a) $X = \pi^0$, $\chi_{\min} = 5\%$. (b) $X = \eta$, $\chi_{\min} = 13\%$. (c) $X = \eta'$, $\chi_{\min} = 20\%$.

for $X = \pi^0$, η , and η' , respectively; here the beam energy was taken as $E_0 = 3$ GeV, and the cutoff parameters θ_{\max} , ψ_{\min} , χ_{\min} , and χ_{\max} were kept fixed at their standard values. It can be seen how the experiment would allow to discriminate (from $\theta' \geq 5^\circ$ on, for all three pseudoscalar particles considered) between the various types of form factors introduced.

V. CONCLUSION

As already stressed in Ref. 1, it would be quite interesting to obtain some indications on the electromagnetic form factors which are effective in the physical region considered (where one of the virtual photons has a high spacelike q^2 value, and the other one may almost be considered as real), all the more since other types of experiments might allow the determination of the same form factors in different physical regions.¹¹

As we see from Table I in Sec. III, the integrated cross sections should be high enough, under the conditions defined, to give rise to reasonably large cross sections in the case of π^0 and η production, provided that electron-positron storage rings with beam energies of 3 GeV or higher, and with a luminosity of at least 10^{32} cm⁻² sec⁻¹ will be available in the future.

On the other hand, the values obtained for η' production are obviously somewhat too low to undertake this type of experiment. The situation would even be worse if the branching ratio $\Gamma(\eta' \rightarrow 2\gamma)/\Gamma(\eta' \rightarrow \text{total})$ proved to be only of the order of 2% (instead of 10%), as a very recent experiment performed at CERN seems to indicate.¹² In that case, one might wonder whether a missing-mass experiment (i.e., a measurement of the outgoing e^\pm particles alone) should not be envisaged for the case of the η' . However, such an experiment would require a special careful preliminary study, since very difficult background problems would arise. Not only the theoretical background (double bremsstrahlung, leptonic processes) but also fortuitous coincidences would have to be taken into account.

As a last remark, we should like to mention that there is an obvious connection between the idea presented here and the suggestion recently made by some other authors^{13,14} to study the deep-inelastic scattering of electrons on a photon target (with multi-hadron production) by looking, here again, for electron-positron inelastic collision processes where one of the e^\pm particles would be scattered at small angle and the other one at large angle. Here again, there will be delicate background problems which should be carefully investigated in the future.

ACKNOWLEDGMENTS

The authors are deeply indebted to Professor J. Haissinski and Professor P. Waloschek for illuminating discussions on the experimental aspects of this study.

They wish also to express their gratitude to Professor M. Morand and Professor F. Perrin for their interest and help.

Finally, they want to thank J. P. Jobez and P. Bonierbale for their technical cooperation.

APPENDIX: DETAILS OF CALCULATION

1. Main Term (Exact Calculation)

The generalized helicity method¹⁵ allows us to write

$$d\sigma = (4\pi\alpha)^6 dC D, \quad (\text{A1})$$

with the kinematic factor dC given by

$$dC = \frac{1}{8(2\pi)^7} \frac{m^6}{E_0^3} d\omega d\tau E' dE' d\Omega d\Omega_k \frac{M^2}{N^2}, \quad (\text{A2})$$

where we use the following symbols: m is the electron mass; E_0 is the beam energy; ω is the lab energy of the left-hand virtual (almost real) photon; $\tau = |q^2|/(4m^2)$, q^2 being the squared four-momentum of the left-hand virtual photon; E' is the lab energy of the right-hand outgoing e^\pm particle (scattered at large angle), and Ω is the solid angle of that particle; Ω_k is the solid angle of one of the emitted photons; M is the invariant mass of the photon pair produced, given by

$$M^2 = 4\omega(E_0 - E') - 2(E_0 - \omega)E'(1 + \cos\Theta), \quad (\text{A3})$$

where Θ is the angle between the outgoing e^\pm particles (it becomes $\Theta \approx \pi - \theta'$ in the case where $\theta \ll \theta'$, θ and θ' being the respective scattering angles of the left-hand and right-hand e^\pm particles). Finally, N is given by

$$N = 2E_0 - (E_0 - \omega)(1 - \cos\psi) - E'(1 - \cos\xi), \quad (\text{A4})$$

where ψ is the emission angle, with respect to the e^\pm colliding-beam axis, of one of the emitted photons, and ξ is the angle between that photon and the right-hand scattered e^\pm particle; the latter angle can be expressed by

$$\cos\xi = -\cos\psi \cos\theta' + \sin\psi \sin\theta' \cos(\Phi - \Phi_k), \quad (\text{A5})$$

where Φ and Φ_k are the respective azimuthal angles of the right-hand scattered e^\pm particle and of the photon considered. [Notice that $d\Phi_k = d\Omega_k/d(\cos\psi)$; and that all angles defined here are taken in the lab frame.]

The dynamic factor D is given by

$$D = \frac{1}{2^9 \pi \alpha^4 m^8} Z F^2 \frac{[\Gamma(X \rightarrow 2\gamma)]^2}{\Gamma(X \rightarrow \text{total})} \delta(M - m_X), \quad (\text{A6})$$

where F is an electromagnetic form factor (for the vertex connecting the particle X with both virtual photons), and Z is expressed as

$$Z = \tau^{-2} \tau'^2 (I_{++}' I_{++}' - I_{+-}' I_{+-}' \cos 2\bar{\Phi}), \quad (\text{A7})$$

with $\tau' = |q'^2|/(4m^2)$, q'^2 being the squared four-momentum of the right-hand virtual photon; I_{++} , I_{+-} are matrix elements of the left-hand virtual photon's polarization matrix, defined in the $\gamma\gamma$ c.m. frame with respect to the $\gamma\gamma$ collision axis; these matrix elements are given by

$$I_{+\pm} = \tau U \pm \tau - 1, \quad (\text{A8})$$

with

$$U = \frac{(8E_0\omega' - M^2 + t' - t)^2}{M^4 + 2(t+t')M^2 + (t-t')^2},$$

where $\omega' = E_0 - E'$, $t = |q^2|$, $t' = |q'^2|$; $I_{+\pm}$ are defined in an entirely similar way for the right-hand virtual photon, and are derived from (A8) by interchanging (t, τ, ω) with (t', τ', ω') . Finally, $\bar{\Phi}$ is the azimuthal angle between the outgoing e^\pm particles in the $\gamma\gamma$ c.m. frame with respect to the $\gamma\gamma$ collision axis. Its expression with respect to the lab parameters is somewhat complicated, but can be derived straightforwardly from formula (A5) of the Appendix of our previous paper.¹

Using formulas (A1)–(A3) and (A6) given above, one gets

$$d\sigma = \frac{\alpha^2}{2^7 \pi^2} \frac{E'}{m^2 E_0^3} \frac{m_X^3}{N^2 N'} Z F^2 \frac{[\Gamma(X-2\gamma)]^2}{\Gamma(X-\text{total})} d\omega d\tau d\Omega d\Omega_k, \quad (\text{A9})$$

where N' is expressed as

$$N' = 2E_0 - (E_0 - \omega)(1 - \cos\Theta) \quad (\text{A10})$$

and E' is given by (A3), substituting m_X for M .

2. Main Term (Williams-Weizsäcker Approximation)

If the Williams-Weizsäcker approximation is applied to the left-hand vertex, one gets

$$d\sigma^{\text{WW}} = \frac{\alpha}{4\pi} \bar{F} \frac{\omega d\omega}{E_0^2} \sigma'(\omega, E_0), \quad (\text{A11})$$

where \bar{F} is the expression given by formula (A10) of the Appendix of Ref. 1 (there it was called F), and σ' is the cross section for the reaction $\gamma e^\pm \rightarrow e^\pm X \rightarrow e^\pm \gamma\gamma$, assuming that the almost real photon of energy ω and the right-hand e^\pm particle of energy E_0 collide practically along the $e^- e^+$ colliding-

beam axis. One easily gets

$$d\sigma' = (4\pi\alpha)^5 dC' D', \quad (\text{A12})$$

$$dC' = \frac{1}{2^{10} \pi^5} \frac{m^2}{\omega E_0} E' dE' d\Omega d\Omega_k \frac{M^2}{N^2}, \quad (\text{A13})$$

$$D' = \frac{1}{2^5 \pi \alpha^4 m^4} (\tau')^{-2} I_{++}'^2 F^2 \frac{[\Gamma(X-2\gamma)]^2}{\Gamma(X-\text{total})} \delta(M - m_X). \quad (\text{A14})$$

All parameters used in (A13) and (A14) have the same definition as in part 1 above, except that I_{++}' now has a somewhat simplified expression:

$$I_{++}' = \tau' \left(\frac{8E_0\omega - M^2 - t'}{M^2 + t'} \right)^2 + \tau' - 1. \quad (\text{A15})$$

One finally gets

$$d\sigma^{\text{WW}} = \frac{\alpha^2}{2^7 \pi^2} \frac{E'}{m^2 E_0^3} \frac{m_X^3}{N^2 N'} \times \bar{F} \frac{I_{++}'^2}{\tau'^2} F^2 \frac{[\Gamma(X-2\gamma)]^2}{\Gamma(X-\text{total})} d\omega d\Omega d\Omega_k, \quad (\text{A16})$$

with N' defined as in part 1, and again E' given by (A3) where m_X is to be substituted for M .

3. Background (Double Bremsstrahlung)

Applying again the Williams-Weizsäcker approximation to the left-hand vertex [this time in the diagram of Fig. 1(b), instead of 1(a)], we write

$$d\sigma^{\text{DB}} = \frac{\alpha}{4\pi} \bar{F} \frac{\omega d\omega}{E_0^2} \sigma^{\text{DC}}(\omega, E_0), \quad (\text{A17})$$

where \bar{F} is again given by formula (A10) of Ref. 1, and σ^{DC} is the cross section for double Compton scattering between an almost real photon of energy ω and an e^\pm particle of energy E_0 , colliding practically along the electron-positron colliding-beam axis.

One then gets

$$d\sigma^{\text{DC}} = (4\pi\alpha)^3 dC' D^{\text{DC}}, \quad (\text{A18})$$

where dC' is again given by (A13), and

$$D^{\text{DC}} = \frac{1}{4} m^{-4} X, \quad (\text{A19})$$

X being used here for a somewhat complicated expression which is given in full detail in formulas (11-33)–(11-35) of Ref. 16. Finally,

$$d\sigma^{\text{DB}} = \frac{\alpha^4}{2^{10} \pi^3} \frac{E'}{m^2 E_0^3} \frac{M^3}{N^2 N'} \bar{F} X dM d\omega d\Omega d\Omega_k, \quad (\text{A20})$$

where E' is to be derived from (A3).

*Work partly supported by the Commissariat à l'Energie Atomique.

¹J. Parisi and P. Kessler, preceding paper, Phys. Rev. D **5**, 2229 (1972).

²N. Arteaga-Romero, A. Jaccarini, P. Kessler, and J. Parisi, Phys. Rev. D **3**, 1569 (1971).

³J. Parisi, N. Arteaga-Romero, A. Jaccarini, and P. Kessler, Phys. Rev. D **4**, 2927 (1971).

⁴J. Parisi, thèse de troisième cycle, Paris, 1970 (unpublished). J. Parisi and P. Kessler, in *Fourth International Symposium on Electron and Photon Interactions at High Energies, Liverpool, 1969*, edited by D. W. Braben and R. E. Rand (Daresbury Nuclear Physics Laboratory, Daresbury, Lancashire, England, 1970), p. 289; unpublished report, 1969. See also: J. Parisi and P. Kessler, Lett. Nuovo Cimento **2**, 760 (1971).

⁵E. J. Williams, Proc. Roy. Soc. (London) **A139**, 163 (1933). C. F. Von Weizsäcker, Z. Physik **88**, 612 (1934). See also: W. Heitler, *The Quantum Theory of Radiation* (Clarendon, Oxford, 1954), 3rd. ed., pp. 414-418; D. Kessler and P. Kessler, Nuovo Cimento **4**, 601 (1956); P. Kessler, Nuovo Cimento **17**, 809 (1961); and Appendix of Ref. 2 above.

⁶Recently, a check of the validity of the Williams-Weizsäcker approximation was performed by S. J. Brodsky, T. Kinoshita, and H. Terazawa [Phys. Rev. D **4**, 1532 (1971)] on the total cross sections of $ee \rightarrow eeX$ (without cuts).

⁷According to electron-positron colliding-beam special-

ists (Professor Haissinski from Orsay and Professor Waloschek from DESY-Hamburg), with whom we discussed this question in detail, such a low angular limit should not be beyond the scope of experimental possibilities.

⁸B. Richter, in *Proceedings of the Fourteenth International Conference on High-Energy Physics, Vienna, 1968*, edited by J. Prentki and J. Steinberger (CERN, Geneva, 1968), pp. 13-14.

⁹Particle Data Group, Rev. Mod. Phys. **43**, S1 (1971); see p. S51.

¹⁰Ref. 9, p. S66.

¹¹There may also be some interest in such a study in connection with recent theoretical work on the light-cone behavior of electromagnetic current commutators [see Y. Georgelin, J. Stern, and J. Jersak, Nucl. Phys. **B27**, 493 (1971)]. The authors are indebted to Dr. Stern for this remark.

¹²M. Basile *et al.*, Nuovo Cimento **3A**, 371 (1971).

¹³T. F. Walsh, Phys. Letters **36B**, 121 (1971).

¹⁴S. J. Brodsky, T. Kinoshita, and H. Terazawa, Phys. Rev. Letters **27**, 280 (1971).

¹⁵P. Kessler, Cahiers Phys. **20**, 55 (1966); Laboratoire de Physique Atomique Report No. PAM 68-05, 1968 (unpublished); Nucl. Phys. **B15**, 253 (1970).

¹⁶J. M. Jauch and F. Rohrlich, *The Theory of Photons and Electrons* (Addison-Wesley, Reading, Mass., 1955), p. 237.

Comparison of the Multiperipheral Model with Inclusive Data in K^+p and π^-p Reactions*

Jerome H. Friedman

Lawrence Berkeley Laboratory, University of California, Berkeley, California 94720

and

Clifford Risk

Lawrence Berkeley Laboratory, University of California, Berkeley, California 94720

and Department of Physics, University of California, Davis, California 95616

(Received 2 December 1971)

The predictions of the multiperipheral model are compared with inclusive data in K^+p and π^-p reactions. We compare with topological longitudinal-momentum distributions, double-differential distributions, multiplicity cross sections, π^+/π^- ratio, asymmetry characteristics, isotropy in the c.m. system, and Regge behavior near the kinematical limit. The agreement is reasonably good. We discuss the relation of this work to earlier work on the multi-Regge model, to results of other models, and to the results obtained by other types of approaches to the inclusive analysis.

I. INTRODUCTION

During the last two years the inclusive^{1,2} type of reaction $a + b \rightarrow c + \text{anything}$ has become a popular means of studying high-energy collisions. Two different approaches to this study can perhaps be

distinguished.

On the one hand, detailed studies have been made of the momentum distribution of particle "c" in the momentum regions near the kinematical limit. For example, comparisons of a given reaction (e.g., $\pi^- + p \rightarrow \pi^- + \text{anything}$ for slow π^- 's in the lab³)